

Tracer Test in Fractured Chalk 2. Numerical Analysis

K.L. Brettmann and K. Høgh Jensen

Technical University of Denmark, Lyngby

R. Jakobsen

Geological Survey of Denmark, Copenhagen

A two-well tracer test carried out in fractured chalk was analyzed using a three-dimensional finite-difference model for flow and transport which, was constructed on the basis of the geological and hydraulic information collected at the field site. The model was developed as a dual-porosity continuum model, in which advection was assumed to occur only in the fractures, and the water in the porous matrix was assumed to be static. The exchange of solute between the fractures (mobile phase) and the porous matrix (immobile phase) was assumed to occur as a diffusion process in response to the local concentration difference of solute between the two phases. Simulations from the dual-porosity model reproduced the shape of the observed breakthrough curves, although some portions of the tail were not accurately represented. The model was also applied as a single-porosity model for advection and dispersion in the fractures with no solute exchange with the porous matrix. The simulations from the single-porosity model greatly overestimated the observed lithium concentrations, and showed very little tailing effect in the falling limb. The study shows that, based on the given tracer test, solute transport in a fractured chalk cannot be represented by a single-porosity approach and hence when dealing with contaminant transport in such systems, both a fractured and a porous domain need to be considered.

Introduction

Transport of non-reactive solutes in groundwater is generally considered to be governed by two principal processes, advection and dispersion. Advection refers to

the mean movement of solute in the flowing groundwater, while dispersion describes the spreading of solute about the mean motion caused by local variations of the groundwater velocity. The classical equation describing the transport of solutes in groundwater is the advection-dispersion equation, which can be written as

$$\frac{\partial C}{\partial t} \equiv = \frac{\partial}{\partial x_i} (v_i C) + \frac{\partial}{\partial x_i} (D_{ij} \frac{\partial C}{\partial x_j}) - S \quad (1)$$

where

C – concentration of the solute

D_{ij} – dispersion coefficient

v_i – pore-water velocity (Darcian flux q divided by porosity n)

S – sink term

The above equation is valid for porous media of constant porosity that are fully saturated in which there is assumed to be no physical or chemical interaction between the fluid and the porous medium, and all of the fluid is assumed to participate in the flow process. However, for many soils and solutes, this is not the case. Solute may be adsorbed onto the soil, or part of the pore water may be stagnant and not participate in the flow process (Gaudet *et al.* 1977).

In a fractured porous medium, the total porosity may be divided into a matrix porosity and a fracture porosity. Matrix porosity generally refers to the intergranular pore space due to grain size and sorting. Fracture porosity is usually due to a secondary process which can be mechanical, such as stress attributed to folding and faulting, or chemical, such as mineralogical alterations or solution channelling. Often, the most rapid groundwater flow takes place in the fractures, which may only account for a small percentage of the overall porosity of the medium. The water stored in the porous matrix may account volumetrically for most of the water in the medium, but it may not significantly contribute to groundwater flow and therefore can be considered as “static” water (Gaudet *et al.* 1977; Bibby 1981). Static water may still play an important role in transport processes by acting as a long-term natural reservoir for solute retention (Lawrence *et al.* 1990). In such situations, the controlling influences on the transport of solutes are not advection and dispersion alone, but also a secondary process of solute diffusion into static water (Bibby 1981).

The effect of static water on mass transport is similar in many ways to the effects produced by solute diffusion into dead-end pores and solute adsorption onto the solids of the porous medium (Bibby 1981). Solute exchange by diffusion can occur between the fractures and the porous matrix at a rate that can depend on several factors, such as the difference in solute concentration between the fracture water and the pore water, and the length of the diffusion paths. Diffusion can significantly attenuate solute concentrations in the fractures (Lawrence *et al.* 1990), as well as increase the retention time of solute in the aquifer. The diffusion of solute from the

static water to the fractures, which occurs when the solute concentration in the fractures declines below the solute concentration in the porous matrix, can also considerably affect solute transport. In this situation, the porous matrix acts as a source of solute to the fractures, sometimes long after the original solute source has been eliminated.

In developing a transport model for fractured or two-domain media, the central issue is whether to model the system as an equivalent porous medium (continuum) or as a discrete fracture network (noncontinuum) (Van Rooy 1987). Of the groundwater models that address transport in fractured media, most treat the aquifer as an equivalent porous medium, see *e.g.* van Genuchten and Wierenga (1976), Grisak and Pickens (1980), and Bibby (1981). Transport models which treat the aquifer as a discrete fracture system are less commonly used for modelling contaminant transport in large-scale groundwater systems. Computational constraints on the total number of fractures that can be included in a discrete network, particularly for three-dimensional systems, limit the applicability of these models to practical large-scale problems. However, as stated by Schwartz and Smith (1988) these models have proven useful in developing concepts of mass transport in fractured rocks. Also, recent field applications to crystalline rock formations have demonstrated that three-dimensional discrete fracture network models may be practical tools for analyzing flow and transport on a scale of a few tens of metres (see *e.g.* Dverstorp and Andersson 1989; Dverstorp *et al.* 1992).

In addition to modelling fluid flow in the fractures, many groundwater transport models have a component which accounts for the exchange of solute between the fractures, or mobile phase, and the pore water, or immobile phase. Many of these solute exchange models are dead-end pore models which assume that the immobile water in the pores is in intimate contact with the mobile water phase (Coats and Smith 1964; Gaudet *et al.* 1977; van Genuchten and Wierenga 1976). These models assume that the diffusion paths are very short, allowing the process to be described by a linear equation. One of the classic linear dead-end pore models was proposed by Coats and Smith (1964)

$$\frac{\partial C_{im}}{\partial t} = \frac{\beta}{n_{im}} (C_m - C_{im}) \quad (2)$$

where

- C_m - concentrations in mobile phase
- C_{im} - concentration in immobile phase
- n_{im} - porosity of porous matrix
- β - diffusion mass transfer coefficient

Other models have been developed in which the mobile and immobile phases are assumed not to be in intimate contact, resulting in a more complicated formulation. Bibby (1981) developed an analytical solution for diffusion in a fractured chalk

aquifer in England that was characterized by relatively large, highly porous blocks of chalk which were separated by narrow fissures. Using an analytical solution for diffusion of a finite mass from a fissure into a porous block, he showed that it may take many days before the rate of mass transfer reduces to an approximately linear form. The model, however, gives rise to a large number of calibration parameters, which requires an extensive amount of data from the aquifer which are normally not available.

The model used in this study for analyzing the results of a tracer study reported by Jakobsen *et al.* (1993) is, as opposed to most previous model analyses of tracer behavior in fractured media, a fully three-dimensional numerical model. The model is based on a continuum approach in which flow and advective transport is assumed to occur only in the fractures, while water in the porous matrix is assumed static. The exchange of mass between the two domains is assumed to take place as solute diffusion.

Numerical Model

To analyze the observed tracer transport in the aquifer over specific vertical intervals, a three-dimensional flow and transport model was constructed based on the available geological and hydraulic information. The model used was the saturated zone module from the European Hydrological System (SHE), which is a finite-difference model based on the governing differential equations for flow and transport in a saturated porous medium (Ammentorp and Refsgaard 1990). In the case of a fractured porous medium, flow and advective transport are assumed to occur only in the fractures. The water in the porous matrix is assumed to be static, such that the porous matrix has no influence on groundwater flow but does affect solute transport by participating in the diffusion of solute between phases.

Groundwater flow in the fractures is based on the governing equation for three-dimensional Darcy-type flow (Freeze and Cherry 1979)

$$S \frac{\partial h}{\partial t} \equiv \frac{\partial}{\partial x} (K_H \frac{\partial h}{\partial x}) + \frac{\partial}{\partial y} (K_H \frac{\partial h}{\partial y}) + \frac{\partial}{\partial z} (K_V \frac{\partial h}{\partial z}) - R \quad (3)$$

where

- h – hydraulic head
- K_H – hydraulic conductivity in horizontal direction
- K_V – hydraulic conductivity in vertical direction
- S – specific storage
- R – sink term
- x, y, z – spatial coordinates
- t – time

Tracer Test in Fractured Chalk 2

In the numerical model this equation is approximated by a set of coupled algebraic equations which are obtained by applying the water balance equation and Darcy's law in finite difference forms to each node in the solution domain assuming that flow occurs in directions between the specific node and its six direct neighbor nodes. The equations are formulated in an implicit scheme where the internode hydraulic conductivity is obtained as the harmonic mean. The system of linear finite difference equations are solved iteratively using a modified Gauss-Seidel method (Thomas 1973).

The transport of solutes in constant density groundwater is described by a form of the advection-dispersion equation which includes a term accounting for the diffusion of solutes between the fractures (mobile phase) and the porous matrix (immobile phase), deMarsily (1986)

$$n_m \frac{\partial C_m}{\partial t} + n_{im} \frac{\partial C_{im}}{\partial t} \equiv - q_i \frac{\partial C_m}{\partial x_i} + n_m \frac{\partial}{\partial x_i} (D_{ij} \frac{\partial C_m}{\partial x_j}) + S \quad (4)$$

where

- C_m - solute concentration in mobile phase
- C_{im} - solute concentration in immobile phase
- n_m - fracture porosity (mobile phase)
- n_{im} - matrix porosity (immobile phase)
- q_i - Darcy flux
- D_{ij} - dispersion coefficient
- S - sink term

The dispersion coefficient is related to the groundwater velocity using Scheidegger's (1961) relationship, which in tensor notation reads

$$D_{ij} = \alpha_{ijm} \frac{u_m u_n}{|u|} \quad i, j, m, n = 1, 2, 3 \quad (5)$$

where

- α - dispersivity
- u - seepage velocity
- $|u|$ - magnitude of seepage velocity

In the general three-dimensional case of arbitrary flow direction in an anisotropic aquifer the dispersion tensor contains 9 components which depend on a dispersivity tensor containing 81 components. Symmetry properties reduce the number of components to 36. A further simplification is obtained if cubic symmetry is assumed in which case the number of components is reduced to 12, Scheidegger (1961).

To reduce the computational burden the numerical formulation has been simplified by neglecting the off-diagonal terms of the dispersion tensor, and hence only the D_{11} , D_{22} and D_{33} components will be accounted for in the numerical solution.

Eliminating the cross-product terms of the dispersion tensor introduces small errors in the solution; yet we consider these errors secondary to the uncertainties present in the field experiment, and the simplified transport description seems justified for an approximate, yet realistic analysis of the tracer experiment.

The components of the dispersivity tensor entering the diagonal components of the dispersion tensor can be grouped into the following four physically recognizable parameters: α_{LH} (longitudinal horizontal dispersivity); α_{TH} (transverse horizontal dispersivity); α_{LV} (longitudinal vertical dispersivity) and α_{TV} (transverse vertical dispersivity).

Hereby, we obtain the following expressions for the diagonal terms

$$\begin{aligned}
 D_{11} &= \alpha_{LH} \frac{u_1 u_1}{|u|} + \alpha_{TH} \frac{u_2 u_2}{|u|} + \alpha_{TV} \frac{u_3 u_3}{|u|} \\
 D_{22} &\equiv \alpha_{TH} \frac{u_1 u_1}{|u|} + \alpha_{LH} \frac{u_2 u_2}{|u|} + \alpha_{TV} \frac{u_3 u_3}{|u|} \\
 D_{33} &\equiv \alpha_{TV} \frac{u_1 u_1}{|u|} + \alpha_{TV} \frac{u_2 u_2}{|u|} + \alpha_{LV} \frac{u_3 u_3}{|u|}
 \end{aligned} \tag{6}$$

Under these assumptions the advection-dispersion equation is solved by finite-difference techniques using an explicit third-order accurate interpolation scheme as described by Vested *et al.* (1992). This scheme is mass-conservative and enables simulation of sharp advective fronts without smearing from numerical dispersion. Due to the explicit formulation the time step is constrained by requirements to maximum allowable advective and dispersive transport distances.

Molecular diffusion is not considered in the model because this process is assumed to be secondary to the dispersive effects introduced by the fairly high flow velocities prevailing during the experiment.

The exchange of mass between the mobile and the immobile water phase as a result of solute diffusion is included in the model as a distributed source/sink term. The approach which has been adopted assumes that the mobile and the immobile waters are in intimate contact and that the diffusion paths are short, and can be described mathematically by

$$n_{im} \frac{\partial C_{im}}{\partial t} = \beta (C_m - C_{im}) \tag{7}$$

where β is the diffusion mass transfer coefficient. This model has been proposed by *e.g.* Coats and Smith (1964), Gaudet *et al.* (1977) and van Genuchten and Wierenga (1976) to model solute diffusion between two domains in the porous medium.

For the purpose of solving the flow and transport equations numerically, a finite-difference grid was developed to represent the model area. In order to minimize the effects of the model boundaries, the flow equation was initially solved over a square grid of approximately 150 m \times 150 m, with a horizontal node spacing of 4

Tracer Test in Fractured Chalk 2

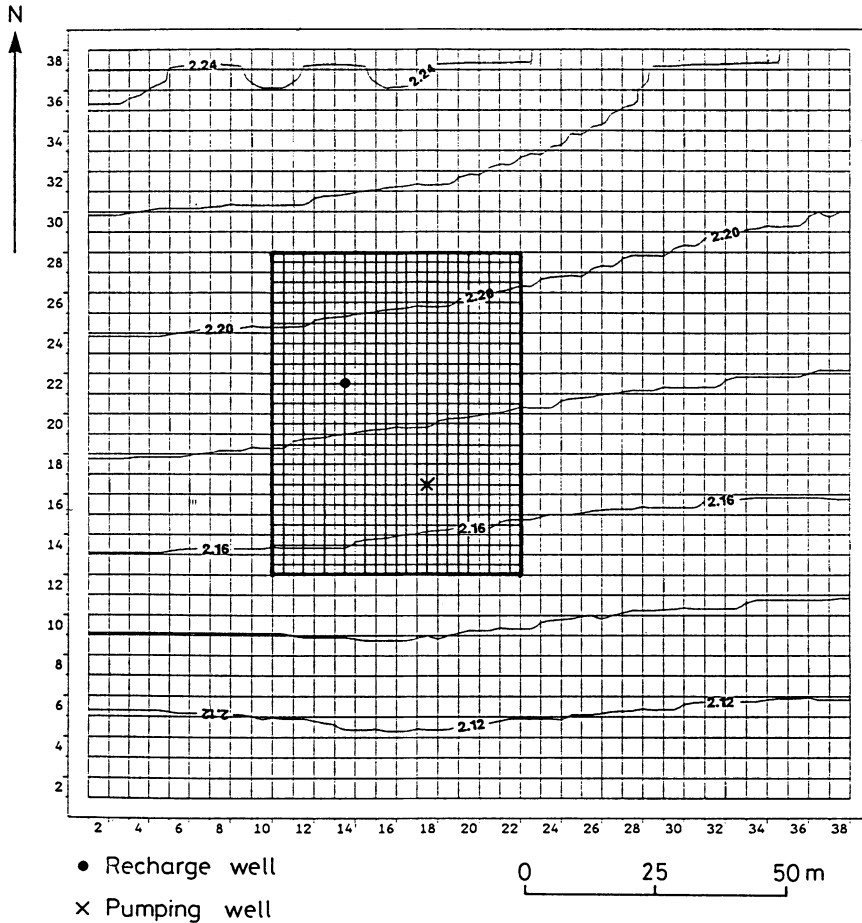


Fig. 1. Horizontal discretization in the numerical model (coarse grid), with the outlined region showing the area over which lithium transport was simulated (fine grid). Hydraulic head values (m) represent simulated conditions prior to the second tracer test.

m. The grid was oriented such that boundary conditions along the vertical planes which bordered the model region were either prescribed head boundaries or no-flow boundaries, depending on the orientation (Fig. 1). The east-west trending boundaries were essentially perpendicular to the natural hydraulic head gradient, and were treated as fixed head boundaries assuming that hydrostatic conditions applied over the vertical extent of the model region. The north-south trending boundaries were parallel to the natural flow lines and were considered no-flow boundaries. Since a finer numerical discretization was desired for transport modeling, a finer grid was developed to cover the immediate test area (Fig. 1). This grid

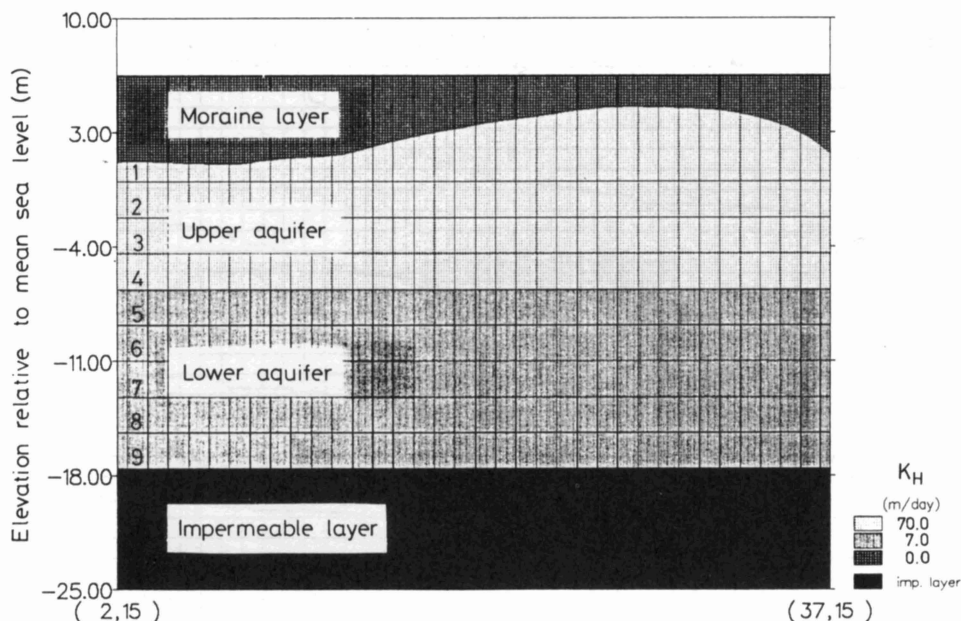


Fig. 2. Vertical discretization of the aquifer in the numerical model.

was 48 by 64 m, and had a horizontal node spacing of 2 m. The boundary conditions used for the fine grid simulation were obtained from the coarse grid solution.

In the vertical plane, the aquifer was represented by nine numerical layers, each with a thickness of 2.2 m (Fig. 2). The upper four layers (8.8 m in total) corresponded to the highly fractured section of the aquifer, and were modelled using a horizontal hydraulic conductivity of 70 m/day. The lower five layers (11.0 m in total) represented the less permeable section of the aquifer, in which a horizontal hydraulic conductivity of 7 m/day was used. The bottom boundary was treated as a no-flow boundary, since very little flow appears to occur in the aquifer below this depth. An additional layer was used in the model to represent the moraine layer. Since the moraine layer has a low permeability, no flow or transport were assumed to occur in this layer such that the aquifer-moraine interface was modelled as a no-flow boundary. Aquifer recharge normally occurs from the vertically downward movement of water through the moraine, but was assumed to be negligible over the short duration of the given test. A timestep of 15 minutes was used for both the flow and transport modelling, which was selected in order to accurately simulate the non-steady nature of the tracer injection.

Simulation Results

In order to define the groundwater velocity field over the region of the tracer test, flow simulation was performed over the coarse numerical grid and subsequently over the fine grid. The pumping and injection rates used in the model were based on the actual rates used during the field test, while the initial values of hydraulic conductivity and specific storage were based on calculated values from the separation injection tests (SIT's) Nilsson and Jakobsen (1990) and the two pump tests, Jakobsen *et al.* (1993). The values representing the two layers in the geological model were slightly adjusted during calibration of the flow model by matching simulated head levels to the observed head levels in the observation wells. Since the lithium transport occurred between wells 7 and 9, it was most important to properly define the velocity field in this region. It was difficult to accurately reproduce the observed head values in all of the wells, so emphasis was placed on reproducing the observed head gradients between the recharge well and the discharge well. Calibration showed that the flow model was most sensitive to the horizontal hydraulic conductivity, although both hydraulic conductivity and storativity were adjusted to achieve a satisfactory calibration of the model. The calibration of the flow model was complicated by the sensitivity of the transport model to the definition of the velocity field between the recharge well and the discharge well. For the final calibration, it was necessary to "iterate" between the flow and transport models in order to achieve a satisfactory calibration of the transport model. The flow model was used to calculate the development in the velocity field over the fine grid for the first 30 hours of the tracer test, after which a steady state velocity field was assumed. This was justified by the small changes in hydraulic head which were observed after 30 hours of pumping. Figs. 3 and 4 show the simulated head levels in the aquifer over the fine numerical grid during and after the lithium injection, respectively.

The transport model was also based on the assumption that the aquifer was composed of two homogeneous layers. Although lithium was detected over the vertical extent of both the recharge and the discharge wells during the test, lithium transport was assumed to occur only through the upper aquifer, based on the assumption that lithium detected in the lowermost interval of the discharge well was transported through the upper interval of the aquifer and upon reaching the well distributed to some degree over the vertical extent of the borehole. As a result, lithium was applied in the numerical model only to the upper aquifer. Based on injection rates and measured lithium concentrations in the injection well, 70 per cent of the total lithium applied in the experiment was assumed to enter the aquifer in the interval corresponding to layers 3 and 4 in the numerical model. The remaining 30 per cent was applied to layers 1 and 2.

For the purpose of determining the appropriate hydraulic parameters to use in the model, it was assumed that the horizontal hydraulic conductivity in the upper

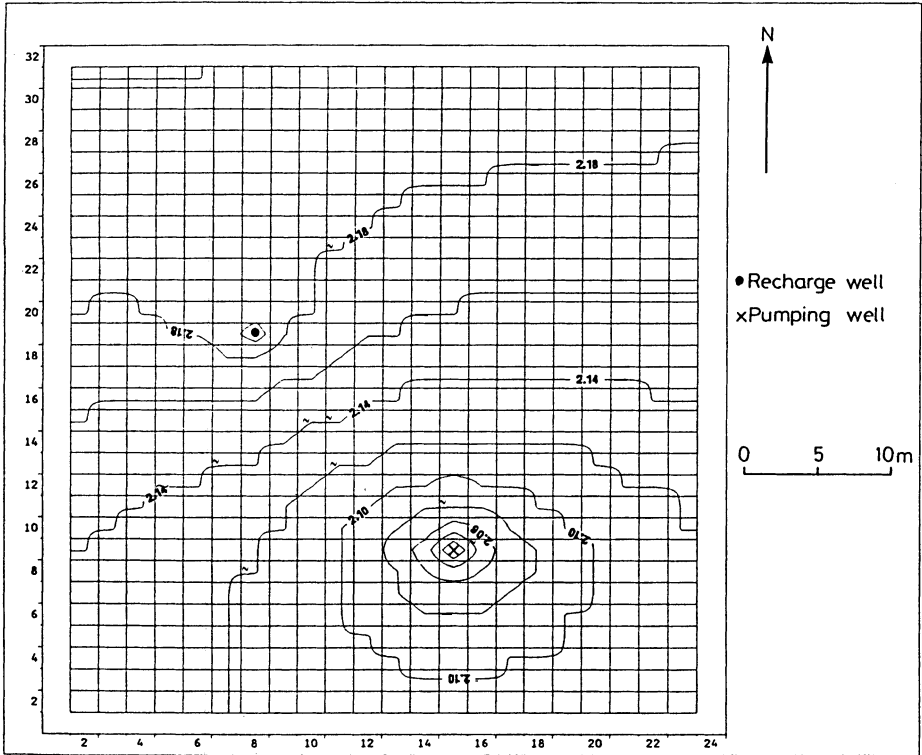


Fig. 3. Simulated hydraulic head levels (m) over the fine finite-difference grid during lithium injection ($t = 7$ hours).

Table 1 = Hydraulic parameters used in the numerical simulations to represent the aquifer

Aquifer level (m)	Numerical layers	K_H (m/d)	K_V (m/d)	Unconfined storativity	Confined storativity
Upper					
Moraine base to -6.6m	4	70.0	1.0	0.016	0.001
Lower					
-6.6 m to -18.0 m	5	7.0	0.14	0.016	0.001

aquifer was 10 times greater than it was in the lower aquifer. This assumption was based on data that were obtained from the separation injection tests. In addition, it was assumed (somewhat arbitrarily) that vertical hydraulic conductivities throughout the aquifer were at least 50 times smaller than the horizontal values. Values for specific storage were used in the model depending on whether confined or unconfined condition existed and were selected based on data obtained from the pump

Tracer Test in Fractured Chalk 2

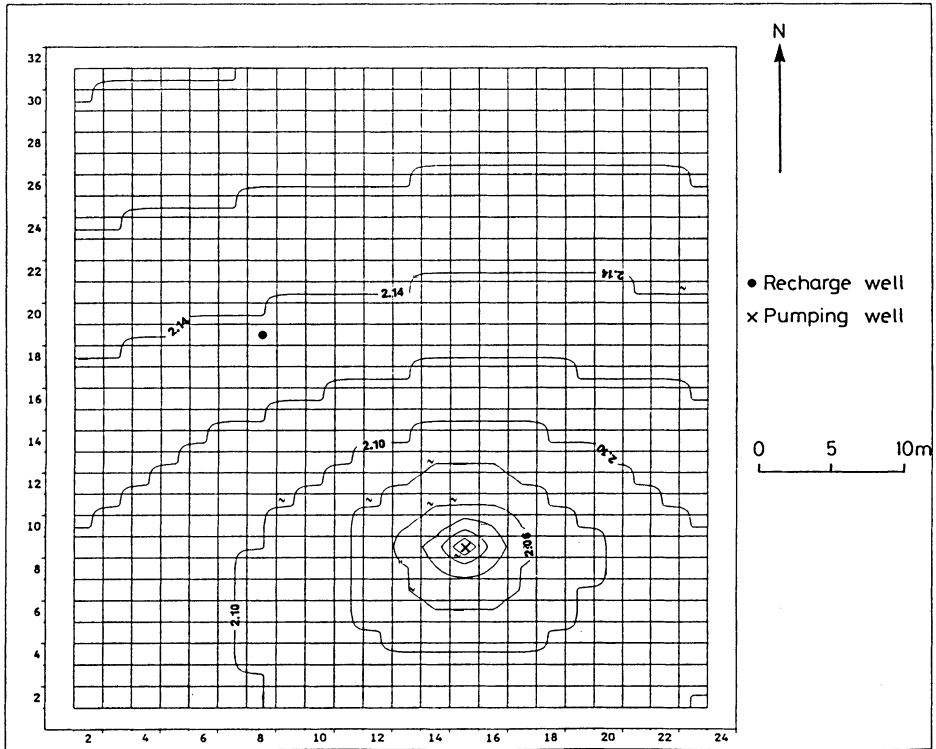


Fig. 4. Simulated hydraulic head levels (m) over the fine finite-difference grid at steady state conditions ($t = 30$ hours).

tests. The hydraulic parameters that were used in the simulations are listed in Table 1.

The transport model was originally developed as a single-porosity model in which transport was assumed to occur only in the fractures due to advection and dispersion. Using a single-porosity approach with a fracture porosity as measured in the field, all attempts to match the simulated breakthrough curves to the observed data were unsuccessful. In all cases the simulated results greatly overestimated the observed lithium concentrations, and were unable to reproduce the long tailing effect observed in the data (Figs. 5, 6 and 7). By assuming that lithium transport occurred only in the fractures, the entire mass of injected lithium moved through the aquifer too rapidly, such that 100 per cent of the injected mass was recovered at the discharge well after only 6 days (144 hours). According to lithium measurements at the discharge well, however, only 47 per cent of the lithium had been recovered after 6 days (see Fig. 8). Furthermore, the single-porosity model would generate transport velocities far too low if the measured matrix porosity was introduced.

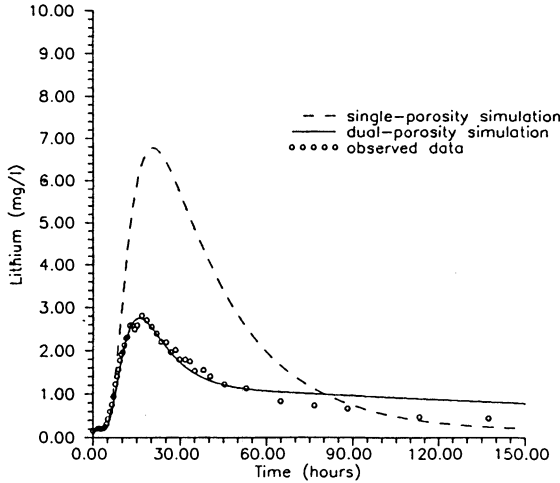


Fig. 5. Comparison of simulated breakthrough curves from the single and dual-porosity models to observed lithium concentrations at the discharge well. The simulated curves correspond to the average output from layers 3 and 4 of the numerical model.

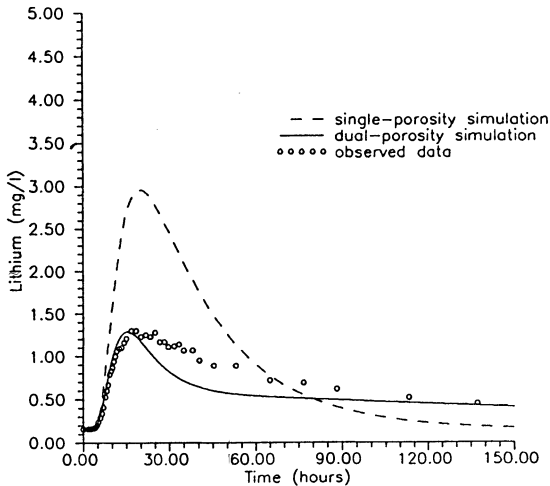


Fig. 6. Comparison of simulated breakthrough curves from the single and the dual-porosity models to observed lithium concentrations at the discharge well. The simulated curves correspond to the output from layer 2 of the numerical model.

After a sharp breakthrough front of the rising limb and peak concentration, the observed breakthrough curves exhibit a long tail of relatively low lithium concentrations which was present throughout the remainder of the test, indicating that some mechanism was retarding the transport of lithium between the wells. This tailing effect was perhaps even more pronounced in the upper intervals of the aquifer, as shown in Figs. 6 and 7.

Tracer Test in Fractured Chalk 2

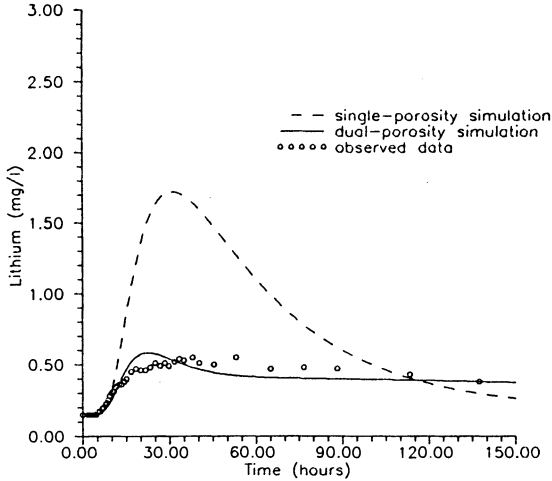


Fig. 7. Comparison of simulated breakthrough curves from the single and the dual-porosity models to observed lithium concentrations at the discharge well. The simulated curves correspond to the output from layer 1 of the numerical model.

Subsequent modelling was based on a dual-porosity approach, in which the porous matrix was represented in the model as a reservoir for solute retention. The exchange of solute between the fractures and the porous matrix was assumed to occur by diffusion in response to local differences in solute concentration between these two phases. The initial simulations that were conducted with the dual-porosity model used parameter values that were based on the observed values for the fracture and matrix porosity, while the dispersivities were taken from the values used in the single-porosity model. The coefficient, β , which controls the rate of solute diffusion between the two phases was used purely as a calibration coefficient.

In order to determine the “best-fit” parameters for the model, the simulated breakthrough curves were fitted to the observed curves for the upper interval of the aquifer by adjusting the values for porosity, longitudinal horizontal dispersivity and β , Figs. 5, 6 and 7. For the three intervals that were simulated, the peak concentration and the rising limb of the curves were reproduced quite well, while on the other hand some portions of the tail were not represented quite as well. Despite some evident problems in the tailing end, the analysis demonstrated that a dual-porosity model provides a much closer representation of the observed transport in the aquifer under investigation than does a single-porosity approach. It may be hypothesized that the simulation problems present in the tailing end could be due to the assumption of an immobile reservoir. If two reservoirs were present with different flow velocities and with little hydraulic connection, the observed tailing effect may have been better described. However, this hypothesis could not be verified on the basis of the available field data.

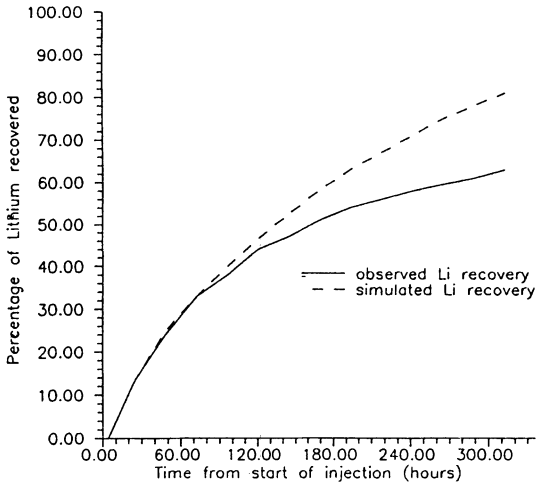


Fig. 8. Comparison of the simulated and the observed percentage of injected lithium recovered at the discharge well vs. time.

Based on the given calibration technique, a set of best-fit parameters were obtained for the dual-porosity transport model. Although some of the parameters were treated as calibration coefficients, others such as the porosity values could be measured directly. For instance, the fracture porosity, which was calibrated to 1.1 per cent in the model, corresponded closely to the spatially averaged value of 1.5 per cent determined from the pump tests. Since advective transport was assumed to occur only in the fractures, the magnitude and the arrival time of the peak concentration were quite sensitive to this parameter, as shown in the results of a sensitivity analysis (Fig. 9). Decreasing the fracture porosity causes a proportionate increase in the groundwater velocities in the fractures, resulting in an earlier breakthrough of the peak concentration. The peak concentration will be higher as a result of a smaller fracture porosity, mainly because less solute dilution will occur in the fractures. Increasing the fracture porosity will have the opposite effect; slower overall travel times and lower peak concentrations.

The sensitivity of the dual-porosity model to the matrix porosity was also investigated (Fig. 10). It is evident that the model is most sensitive to this parameter at low values. The matrix porosity appeared to have no effect on the initial breakthrough front, although it had a slight effect on the peak breakthrough concentration and a significant effect on the tail of the breakthrough curve. As the amount of matrix porosity that is involved in solute exchange becomes greater, a larger amount of solute will initially diffuse to the matrix in an attempt to achieve solute equilibrium between the phases. This will result in more of the solute being stored in the matrix, such that the tail following the initial breakthrough pulse will have a relatively low concentration but will continue for a long duration as the solute slowly diffuses back to the fractures. Conversely, as the matrix porosity becomes

Tracer Test in Fractured Chalk 2

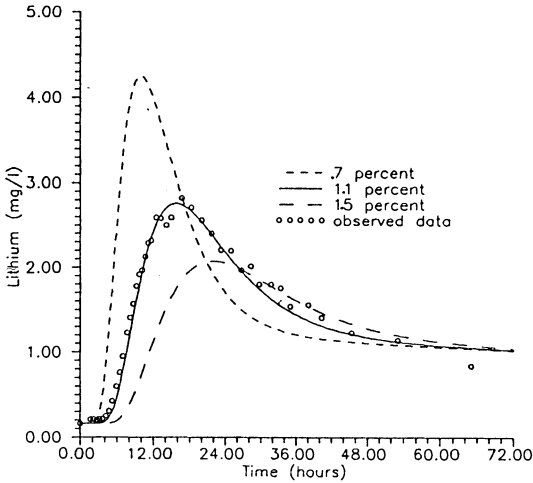


Fig. 9. Sensitivity of the simulated breakthrough curve (layers 3 and 4) from the dual-porosity model to the fracture porosity of the aquifer.

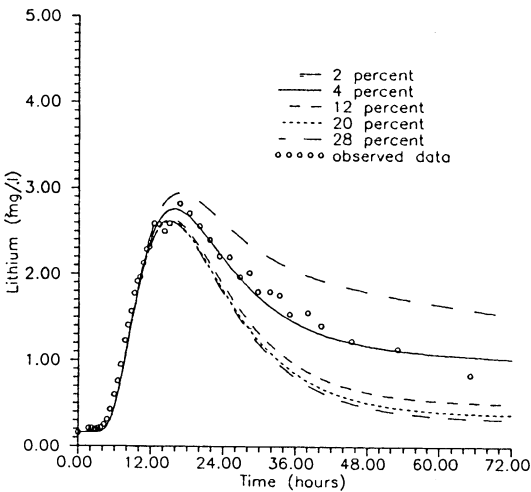


Fig. 10. Sensitivity of the simulated breakthrough curve (layers 3 and 4) from the dual-porosity model to the matrix porosity which is actively involved in solute diffusion.

smaller, less solute will diffuse to the matrix in an attempt to achieve solute equilibrium. More of the solute in this case will pass through the fractures with the initial pulse, resulting in breakthrough curves with higher overall concentrations and shorter duration tails.

As seen from the sensitivity analysis, the calibrated value for the matrix porosity was 4 per cent, which is significantly lower than the values suggested by core analysis (20-35 per cent). Although this result could indicate that the simple linear solute exchange model is insufficient for the studied aquifer, the physical signifi-

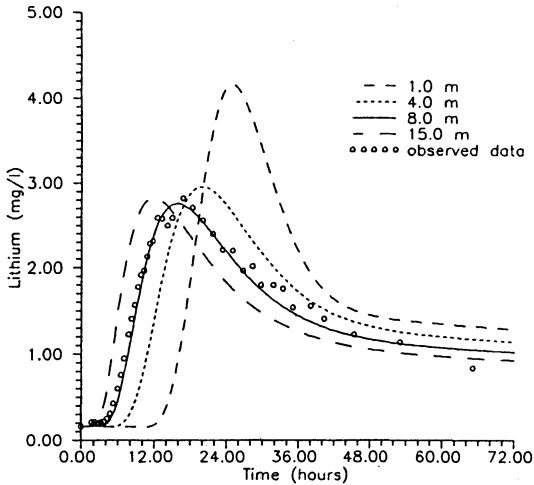


Fig. 11. Sensitivity of the simulated breakthrough curve (layers 3 and 4) from the dual-porosity model to the longitudinal horizontal dispersivity, α_{LH} .

cance of such a small matrix porosity may be justified, if one considers that this value does not necessarily represent the entire matrix porosity, but rather the matrix porosity that is “actively” involved in solute diffusion. Considering the short duration of the test, it seems reasonable that only a fraction of the total matrix porosity was involved in the diffusion process. This would most likely represent the pores that are in closest contact with the fractures. Unfortunately, it was not possible to confirm this hypothesis with field or laboratory measurements, so the physical validity of this value remains unclear.

The dispersivity values that were used in the initial simulations were based partly on the calculated dispersivities for a fractured chalk at Dorset, England that are reported in a review by Gelhar *et al.* (1985). A sensitivity analysis was subsequently conducted in order to identify the dispersivity values which most closely reproduced the observed breakthrough curves. Based on this analysis, the simulated breakthrough curves appear to be quite sensitive to particularly the longitudinal horizontal dispersivity (Fig. 11). Since this parameter controls how much the lithium plume will spread, it is an important parameter for determining when the initial breakthrough of lithium will occur. Also the peak concentration of the breakthrough curve is sensitive to this parameter.

The dispersivities in the vertical direction appeared to have minor effect on the simulation results and therefore it was not possible to identify these parameters very accurately on the basis of the present experiment. During the calibration of the transport model, the dispersivities in the horizontal direction were adjusted in order to fit the peak and the rising limb of the simulated breakthrough curve to the observed data. On the basis of calibration, the “best-fit” dispersivities were determined to be: $\alpha_{LH} = 8.0$ m, $\alpha_{TH} = 0.05$ m, $\alpha_{LV} = 0.001$ m, and $\alpha_{TV} = 0.001$ m.

Tracer Test in Fractured Chalk 2

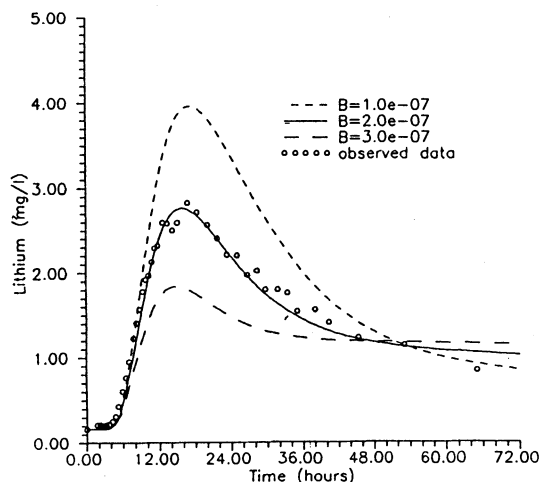


Fig. 12. Sensitivity of the simulated breakthrough curve (layers 3 and 4) from the dual-porosity model to the diffusion mass transfer coefficient, β .

The longitudinal horizontal dispersivity, α_{LH} , appears to be very high, especially at the scale of the test (25 m). Yet, this value compares reasonably well with the dispersivities reported in Gelhar *et al.* (1985) and with the results from a similar tracer test reported by Stephenson *et al.* (1989). The high value for the longitudinal dispersivity parameter obtained in the calibration process is caused by the dispersion arising from the heterogeneity of the discontinuously-fractured aquifer not accounted for in the flow model. Perhaps the heterogeneity introduced by the random fracture orientation in the chalk at least partly accounts for the large value of α_{LH} . As it is always the case in dispersion analyses, if the data permits a more detailed description of the spatial variation of the flow lines, a smaller dispersivity parameter would result.

The diffusion mass transfer coefficient, β , is an empirical parameter which was determined to have an optimal value of $2.0 \times 10^{-7} \text{ d}^{-1}$ based on curve-fitting. As shown in Fig. 12, the simulated breakthrough curves are very sensitive to this parameter, since it controls the rate of solute exchange between the mobile and the immobile water phases. As β is increased, solute diffusion takes place at a faster rate, which causes a more rapid attenuation of the peak solute concentrations in the fractures. The effect is to shift more of the solute mass to the tail of the breakthrough curve, such that a relatively high concentration and long duration tail is obtained. Decreasing β decreases the rate of diffusion, which diminishes the effect that solute diffusion has on the overall transport process for a short-duration tracer test.

In order to better understand the mechanisms involved in lithium transport through the aquifer, a comparison can be made between the simulated breakthrough curves and the observed data (Figs. 5, 6 and 7). Based on the results of the

simulations, it is quite evident that the lithium mass moves through the aquifer at a much slower rate than can be accounted for by a single-porosity model. The main effect of lithium diffusion into the porous matrix is to retard the transport of lithium through the aquifer. In the dual-porosity model, the slow movement of lithium through the aquifer can be explained by an initially rapid diffusive exchange of lithium between the fractures and the porous matrix, and the subsequent retention of this lithium in the matrix. According to simulation from the dual-porosity model, most of the lithium was transferred to the porous matrix shortly after injection, such that 81 per cent of the lithium remaining in the aquifer after 2 days was stored in the matrix. This lithium remained in the matrix until the concentration gradient was favorable for it to diffuse from the matrix to the fractures which at least partly explains the observed tailing effect on the breakthrough curves.

Another mechanism which may affect lithium transport is the adsorption of lithium onto the aquifer material. Lithium has been shown to be a reactive tracer in other field tests, one of the best examples being the Cape Cod tracer test (LeBlanc *et al.* 1991) in which lithium transport was shown to be retarded when compared with the non-reactive tracer, bromide. Laboratory experiments by Wood *et al.* (1990) suggest that for the Cape Cod study, the majority of the reaction sites for lithium were in grain interiors, such that most reactions were preceded by lithium diffusion into the aquifer material. The study by LeBlanc *et al.* (1991) also suggests that although lithium may be acting as a reactive substance, this effect is not seen immediately. A comparison of the movement of bromide and lithium at the Cape Cod site showed that as late as 33 days after the tracer injection, there was little difference in the areal distribution of the two plumes. Although the retardation effect depends on the specific aquifer material, the observations at the Cape Cod site seem to suggest that the reaction of lithium was not a significant factor during the earlier stages of the present test. Since the Karlstrup test lasted only 21 days, it seems possible that any adsorption effects would have been overshadowed by the initial diffusion of lithium into the matrix. Adsorption might have been somewhat more significant during the later stages of the tracer test, and it could partly account for more lithium remaining in the aquifer than was calculated by the dual-porosity model (see Fig. 8).

Conclusions

A two-well tracer test using lithium chloride was conducted in a fractured chalk aquifer as a means to investigate solute transport in a fractured porous medium typical of the geological conditions in Denmark. To better understand the transport processes involved, a numerical flow and transport model was constructed to simulate the field test. The model was originally applied using a single-porosity continuum approach, but was later modified to a dual-porosity continuum model to simulate solute diffusion between the fractures and the porous matrix. Solute diffusion was assumed to occur as a linear process in response to the local concentration differences of solute between the two phases.

The parameter values used in the models were based on measured hydraulic parameters as well as calibrated values that were obtained by fitting simulated breakthrough curves to the observed data. The simulations using the single-porosity model greatly overestimated the observed lithium concentrations, and were unable to reproduce the long tail observed on the falling limb of the observed breakthrough curves. Simulations using a dual-porosity approach, on the other hand, better reproduced the shape of the observed breakthrough curves, although some portions of the tail were not accurately represented. A sensitivity analysis was subsequently conducted in order to determine the sensitivity of the model to selected parameters.

Based on the observed data and the simulated results, it is apparent that solute transport in the studied chalk aquifer cannot be represented by a single-porosity approach. Although most of the groundwater flow and hence advective transport may take place in the fractures, mass transport appears to be controlled, at least initially, by the solute diffusion between the fractures and the essentially static water in the porous matrix. Depending on the amount of matrix porosity that is actively involved in the diffusion process, a significant amount of solute can diffuse to the porous matrix and remain in storage until the local concentration gradient favors reverse diffusion back to the fractures. This process can significantly attenuate the peak solute concentrations in the fractures, as well as greatly increase the retention time of solute in the aquifer.

On the basis of the simulation results it is hypothesized that only a portion of the total matrix porosity may be actively involved in solute diffusion at least for the time span considered, although no field measurements have been made to confirm this. The most favorable simulation results were obtained using a matrix porosity of 4 per cent, which is considerably lower than the values of 20 to 35 per cent that were determined by core analysis. Based on the relatively short time scale of the given test, it seems possible that only the pores in closest contact with the fractures participated in the diffusive exchange of solute.

Another mechanism which may affect lithium transport is the adsorption of lithium ions onto the aquifer material. Although adsorption was not considered in

the present study, past field tests have shown lithium to be a reactive tracer. It is likely that adsorption may have been an important process during the later stages of the Karlstrup test, although solute diffusion appears to be the dominant process during the earlier stages of the test. It is evident that larger-scale tracer investigations involving conservative and non-conservative tracers are needed in the future in order to better understand the effects of solute advection, dispersion and reaction in a fractured chalk. The present study does, however, show that when dealing with contaminant transport in a fractured medium, both a fractured and a porous domain need to be considered.

Acknowledgements

The numerical investigations that were performed by the first author were made possible by a research grant provided by the Valle Scholarship and Scandinavian Exchange Program at the University of Washington, Seattle. The first author is deeply grateful to the Valle Program for the opportunity to work as a visiting scientist at the Technical University of Denmark while this research was conducted. The Danish Hydraulic Institute is acknowledged for supporting the application of the SHE-model.

References

- Ammentorp, H.C., and Refsgaard, A. (1991) Operationalisation of a three-dimensional model, Report 174/177, Landfill project, Danish Environmental Protection Agency, Copenhagen, 88 pp.
- Bibby, R. (1981) Mass transport of solutes in dual-porosity media, *Water Resour. Res.*, Vol. 17(4), pp. 1075-1081.
- Coats, K.H., and Smith, B.D. (1964) Dead-end pore volume and dispersion in porous media, *Society of Petroleum Engineers Journal*, Vol. 3, pp. 73-84.
- deMarsily, G. (1986) *Quantitative hydrogeology, Groundwater hydrology for engineers*, Academic Press, Inc..
- Dverstorp, B., and Andersson, J. (1989) Application of the discrete fracture network concept with field data: Possibilities of model calibration and validation, *Water Resour. Res.* Vol. 25(3), pp. 540-550.
- Dverstorp, B., Andersson, J., and Nordqvist, W. (1992) Discrete fracture network interpretation of field tracer migration in sparsely fractured rock, *Water Resour. Res.*, Vol. 28(9), pp. 2327-2343.
- Freeze, R.A., and Cherry, J.A. (1979) *Groundwater*, Prentice-Hall, Englewood Cliffs, New Jersey, USA.

Tracer Test in Fractured Chalk 2

- Gaudet, J.P., Jegat, H., Vachaud, G., and Wierenga, P.J. (1977) Solute transfer, with exchange between mobile and stagnant water, through unsaturated sand, *Soil Science Society of America Journal*, Vol. 41(4), pp. 665-671.
- Gelhar, L.W., Mantoglou, A., Welty, C., and Rehfeldt, K.R. (1985) A review of field-scale physical solute processes in saturated and unsaturated porous media, Electric Power Research Institute, Report EA-4190.
- Grisak, G.E., and Pickens, J.F. (1980) Solute transport through fractured media 1. The effect of matrix diffusion, *Water Resour. Res.*, Vol. 16(4), pp. 719-730.
- Jakobsen, R., Jensen, K. Høgh, and Brettmann, K.L. (1993) Tracer test in fractured chalk, 1. Experimental design and results, *Nordic Hydrology*, Vol. 24(2/3), pp. 263.
- Lawrence, A.R., Chilton, P.J., Barron, R.J., and Thomas, W.M. (1990) A method for determining volatile organic solvents in chalk pore waters (southern and eastern England) and its relevance to the evaluation of groundwater contamination, *J. Contam. Hydrol.*, Vol. 6, pp. 377-386.
- LeBlanc, D.R., Garabedian, S.P., Hess, K.M., Gelhar, L.W., Quadri, R.D., Stollenwerk, K.G., and Wood, W.W. (1991) Large-scale natural gradient tracer test in sand and gravel, Cape Cod, Massachusetts, 1, Experimental design and observed tracer movement, *Water Resour. Res.*, Vol. 27(5), pp. 895-910.
- Nilsson, B., and Jakobsen, R. (1990) The separation pumping technique, Proc. the NATO/CCMS pilot study on demonstration of remedial action techniques for contaminated land and groundwater, Fourth international conference, Angers, France.
- Schleidegger, A.E. (1961) General theory of dispersion in porous media, *Jour. Geophys. Research*, Vol. 66(10), pp. 3273-3278.
- Schwartz, F.W., and Smith, L. (1988) A continuum approach for modeling mass transport in fractured media, *Water Resour. Res.*, Vol. 24(8), pp. 1360-1372.
- Stephenson, D., Paling, W.A.J., and De Jesus, A.S.H. (1989) Radiotracer dispersion tests in a fissured aquifer, *J. Hydrol.*, Vol. 110, pp. 153-164.
- Thomas, R.G. (1973) Groundwater models. Irrigation and drainage, Spec. Paper, Food and Agricultural Organization, No. 21, U.N., Rome.
- Van Genuchten, M. Th., and Wierenga, P.J. (1976) Numerical solution for convective dispersion with intra-aggregate diffusion and non-linear adsorption, in *System Simulation in Water Resources*, edited by G.C. Vansteenkiste, North-Holland, Amsterdam, p. 275.
- Van Rooy, D. (1987) Transport in fractured rock (Literature review), Danish Landfill Project, Status report M3, Institute of Hydrodynamics and Hydraulic Engineering, Technical University of Denmark.
- Vested, H.J., Justesen, P., and Ekebjærg, L. (1992) Advection-diffusion modelling in three dimensions, *Applied Mathematical Modelling*, Vol. 12, pp. 506-519.
- Wood, W.W., Kraemer, T.F., and Hearn, P.P. (1990) Intragranular diffusion: An important mechanism influencing solute transport in clastic aquifers, *Science*, Vol. 247, pp. 1569-1572.

First received: 17 February, 1993

Revised version received: 24 May, 1993

Accepted: 27 May, 1993

Address:

K.L. Brettmann,
K. Høgh Jensen,
Institute of Hydrodynamics and
Hydraulic Engineering (ISVA),
Technical University of Denmark,
Building 115,
DK-2800 Lyngby, Denmark.

R. Jakobsen,
Geological Survey of Denmark,
Thoravej 8,
DK-2400 Copenhagen NV,
Denmark.